Journal of Computations & Modelling, vol.3, no.4, 2013, 287-309
ISSN: 1792-7625 (print), 1792-8850 (online)
Scienpress Ltd, 2013

Simulation study of the modification of the high-latitude ionosphere by powerful high-frequency radio waves

G.I. Mingaleva[1] and V.S. Mingalev[1]

Abstract

A mathematical model of the high-latitude ionosphere, developed earlier in the Polar Geophysical Institute, is utilized to calculate three-dimensional distributions of ionospheric parameters, modified by the action of the ionospheric heater. The model takes into account the convection of the ionospheric plasma, strong magnetization of the plasma at F-layer altitudes, and geomagnetic field declination. The calculations were made for two cases. Firstly, we simulated the distributions of the ionospheric parameters under natural conditions without a powerful high-frequency wave effect. Secondly, the distributions of the ionospheric parameters were calculated on condition that an ionospheric heater, situated at the point with geographic coordinates of the HF heating facility near Tromso, Scandinavia, has been operated, with the ionospheric heater being located on the night side of the Earth. The results of the numerical simulation indicate that

1 Polar Geophysical Institute of the Kola Scientific Center, Russian Academy of Sciences, Apatity 184209, Murmansk Region, Russia. E-mail: mingalev@pgia.ru

Article Info: *Received* : September 23, 2013. *Revised* : October 31, 2013.
Published online : December 1, 2013.

artificial heating of the ionosphere by powerful high-frequency waves ought to influence noticeably on the spatial structure of the nighttime high-latitude F-region ionosphere in the vicinity of the ionospheric heater.

Mathematics Subject Classification: 65Z05
Keywords: High-latitude ionosphere; Active experiments; Modeling and forecasting; Plasma temperature and density

1 Introduction

Experiments with high-power, high-frequency radio waves were successfully used for the investigation of the ionospheric plasma's properties during the last four decades. For this investigation, some high-power radio wave heaters have been built over the world. The majority of these heaters have been built in the mid-latitudes (Platteville, Arecibo, Nizhny Novgorod, etc.). However, a few ionospheric heaters have been applied for investigation of the high-latitude ionosphere owing to their location in the high-latitudes, in particular, near Tromso, Scandinavia. These experiments indicate that high-power high-frequency (HF) radio waves, pumped into the ionosphere, cause the variety of physical processes in the ionospheric plasma. Some of such processes can result in the disturbances of the height profiles of the ionospheric parameters at F-layer altitudes (above approximately 150 km). Experiments with high-power, high-frequency radio waves, used for the investigation of the ionospheric plasma's properties during the last four decades, indicated that powerful HF waves can produce significant large-scale variations in the electron temperatures and densities at F-layer altitudes [1 - 18].

To investigate the response of the high-latitude F region to a powerful HF wave and the role of specific features of the high-latitude ionosphere, mathematical models may be utilized. To date very few mathematical models of

the high-latitude F region, which can be affected by a powerful HF wave, have been developed. One of such mathematical models has been developed in the Polar Geophysical Institute [19]. This model has been used to simulate the influence of the frequency, power, and modulation regime of the HF waves on the expected response of the height profiles of the ionospheric parameters at F-layer altitudes to HF heating [20 - 24].

It may be expected that the large-scale disturbances, caused by artificial heating, can cover some area in the horizontal plane. To study the dimension of this area the numerical modeling can be applied. The purpose of this paper is to examine how high-power high-frequency radio waves, pumped into the high-latitude ionosphere, influence on the ionospheric parameters distributions in the horizontal directions at F-layer altitudes.

2 Numerical model

2.1 Three-dimensional mathematical model of the high-latitude ionosphere

In the present study, to calculate three-dimensional distributions of the ionospheric parameters in the F-region ionosphere the mathematical model of the convecting high-latitude ionosphere, developed earlier [25, 26], is applied. The model produces three-dimensional distributions of the electron density, positive ion velocity, and ion and electron temperatures. It encompasses the ionosphere above 36^0 magnetic latitude and at distances between 100 and 700 km from the Earth along the magnetic field line for one complete day. The applied numerical model takes into consideration the strong magnetization of the plasma at F-layer altitudes and the attachment of the charged particles of the F-region ionosphere to the magnetic field lines. As a consequence, the F-layer ionosphere plasma drift in the direction perpendicular to the magnetic field **B** is strongly affected by the

electric field **E** and follows **E×B** convection paths (or the flow trajectories). In the model calculations, a part of the magnetic field tube of the ionospheric plasma is considered at distances between 100-700 km from the Earth along the magnetic field line. The temporal history is traced of the ionospheric plasma included in this part of the magnetic field tube moving along the flow trajectory through a neutral atmosphere. By tracing many field tubes of plasma along a set of flow trajectories, we can construct three-dimensional distributions of ionospheric quantities.

As a consequence of the strong magnetization of plasma at F-layer altitudes, its motion may be separated into two flows: the first, plasma flow parallel to the magnetic field; the second, plasma drift in the direction perpendicular to the magnetic field. The parallel plasma flow in the considered part of the magnetic field tube is described by the system of transport equations, which consists of the continuity equation, the equation of motion for ion gas, and heat conduction equations for ion and electron gases. These equations in the reference frame, convecting together with a field tube of plasma, whose axis *h* is directed upwards along the magnetic field line, may be written as follows:

$$\frac{\partial N}{\partial t}+\frac{\partial}{\partial h}(NV_i)=q+q_e+q_p-l\,, \tag{1}$$

$$\begin{aligned} m_iN\Big(\frac{\partial V_i}{\partial t}+V_i\frac{\partial V_i}{\partial h}\Big)-\frac{4}{3}\frac{\partial}{\partial h}\Big(\mu\frac{\partial V_i}{\partial h}\Big)+\frac{\partial}{\partial h}[N\kappa(T_i+T_e)]+m_iNg\sin I \\ =m_iN\sum_{n=1}^{3}\frac{1}{\tau_{in}}(U_n-V_i)\,, \end{aligned} \tag{2}$$

$$\frac{\partial T_i}{\partial t}=\frac{1}{M}\frac{\partial}{\partial h}\Big(\lambda_i\frac{\partial T_i}{\partial h}\Big)-V_i\frac{\partial T_i}{\partial h}+\frac{\gamma-1}{N}\Big(\frac{\partial N}{\partial t}+V_i\frac{\partial N}{\partial h}\Big)T_i+\frac{1}{M}\Big(P_{ie}+\sum_{n=1}^{3}P_{in}\Big), \tag{3}$$

$$\begin{aligned} \frac{\partial T_e}{\partial t}=\frac{1}{M}\frac{\partial}{\partial h}\Big(\lambda_e\frac{\partial T_e}{\partial h}\Big)-V_e\frac{\partial T_e}{\partial h}+\frac{\gamma-1}{N}\Big(\frac{\partial N}{\partial t}+V_e\frac{\partial N}{\partial h}\Big)T_e \\ +\frac{1}{M}\Big(P_{ei}+\sum_{n=1}^{3}P_{en}+Q+Q_e+Q_p+Q_f-L_r-L_v-L_e-L_f\Big) \end{aligned} \tag{4}$$

where N is the O^+ ion number density (which is assumed to be equal to the

electron density at the F-layer altitudes); V_i is the parallel (to the magnetic field) component of the positive ion velocity; q is the photoionization rate; q_e is the production rate due to auroral electron bombardment; q_p is the production rate due to auroral proton bombardment; l is the positive ion loss rate (taking into account the chemical reactions

$O^+ + O_2 \rightarrow O_2^+ + O,$

$O^+ + N_2 \rightarrow NO^+ + N,$

$O_2^+ + e \rightarrow O + O,$ and

$NO^+ + e \rightarrow N + O$);

m_i is the positive ion mass; k is Boltzmann's constant; T_i and T_e are the ion and electron temperatures, respectively; g is the acceleration due to gravity; I is the magnetic field dip angle; $1/\tau_{in}$ is the collision frequency between ion and neutral particles of type n ; U_n is the parallel component of velocity of neutral particles of type n; $M = \frac{3}{2}\kappa N$, $\gamma = \frac{5}{3}$; V_e is the parallel component of electron velocity (which is determined from the equation for parallel current); μ is the ion viscosity coefficient; λ_i and λ_e are the ion and electron thermal conductivity coefficients; Q , Q_e , Q_p and Q_f are the electron heating rates due to photoionization, auroral electron bombardment, auroral proton bombardment, and HF heating, respectively; L_r, L_v, L_e and L_f are the electron cooling rates due to rotational excitation of molecules O_2 and N_2, vibrational excitation of molecules O_2 and N_2, electronic excitation of atoms O, and fine structure excitation of atoms O, respectively.

The quantities on the right-hand sides of equations (3) and (4), denoted by P_{ab}, describe the type a particles energy change rates as a result of elastic collisions with particles of type b, with large drift velocity differences having been taken into account. Thus, the quantities P_{ab} contain the frictional heating produced by electric fields and thermospheric winds. Concrete expressions of the model parameters that appear in the Eqs.(1-4) are the same as in the papers by Mingaleva

and Mingalev [25, 26].

The plasma drift in the direction perpendicular to the magnetic field coincides with the motion of the magnetic field tube along the flow trajectory which may be obtained using the plasma convection pattern. The use of plasma convection pattern allows us not only to obtain the configurations of the flow trajectories but also to calculate the plasma drift velocity along them at an F-layer altitude. It is known that the convection trajectories, around which the magnetic field tubes are carried over the high-latitude region, are closed for a steady convection pattern. For each flow trajectory, we obtain variations of ionospheric quantities with time (along the flow trajectory), that is, the profiles against distance from the Earth along the geomagnetic field line of the electron density, positive ion velocity, and electron and ion temperatures are obtained by solving the system of transport equations of ionospheric plasma, described above. These profiles result in two-dimensional steady distributions of ionospheric quantities along the each flow trajectory. By tracing many field tubes of plasma along a set of convection trajectories, we can construct three-dimensional distributions of ionospheric quantities.

The neutral atmosphere composition, input parameters of the model, numerical method, and boundary conditions were in detail described in the studies by Mingaleva and Mingalev [25, 26].

2.2 Calculations of artificial heating of the ionosphere

It is known that the energy absorption of a powerful HF wave in the ionosphere can take place due to various linear and nonlinear processes. The applied model is intended to investigate how the absorbed energy of HF wave influences on the large-scale F-region modification. One of the important physical parameter is the effective absorbed power (EAP). It is known that the EAP is connected with the effective radiated power (ERP) by the formula

$$EAP = \eta \cdot ERP \quad (5)$$

where η is the coefficient characterizing the fraction of the energy of the powerful HF wave deposited in the ambient electron gas and lost for its heating. In the concrete ionospheric heating experiment, the value of the coefficient η is not known exactly. Moreover, distinct high-power radio wave heaters can provide different values of the ERP. Therefore, in various ionospheric heating experiments, the values of the EAP may be different. Therefore, the EAP is chosen as an input parameter of the mathematical model.

The applied mathematical model takes into account the following heating mechanism, caused by the action of the powerful HF radio waves. The absorption of the heater wave energy is supposed to give rise to the formation of field-aligned plasma irregularities on a wide range of spatial scales. In particular, short-scale field-aligned irregularities are excited in the electron hybrid resonance region. These irregularities are responsible for the anomalous absorption of the electromagnetic heating wave (pump) passing through the instability region and cause anomalous heating of the plasma. The rate of this anomalous heating is denoted by Q_f and included in the heat conduction equation for electron gas, Eq.(4). The concrete expression to the Q_f, containing the EAP, was taken from the study by Blaunshtein et al. [27]. This expression was in detail reproduced in the studies by Mingaleva and Mingalev [19] and Mingaleva et al. [24]. It can be noted that this rate of anomalous heating is directly proportional to the EAP. Consequently, a necessity of knowledge of the precise value of the coefficient η, present in Eq.(5), is absent. In the utilized model, the EAP is the input parameter of the model. The utilized expression of the rate of anomalous heating, in spite of its simplicity, allows us to evaluate approximately the influence of artificial heating of the ionosphere on the expected large-scale F-region modification.

In the present study, the electric field distribution, which is the combination of the pattern B of the empirical models of high-latitude electric fields of Heppner [28] and the empirical model of ionospheric electric fields at middle latitudes,

developed by Richmond [29] and Richmond et al. [30], is utilized. The utilized electric field distribution is a steady non-substorm convection model. Using this convection model, we calculate the plasma drift velocity along the convection trajectories, which intersect the F-layer volume illuminated by an ionospheric heater situated at the point with geographic coordinates of the HF heating facility near Tromso, Scandinavia. For these convection trajectories, we obtain variations of profiles against distance from the Earth along the geomagnetic field line of the ionospheric quantities with time (along the trajectory) by solving the system of transport equations described above. These profiles result in two-dimensional distributions of ionospheric quantities along the each flow trajectory. Using these two-dimensional distributions along the each convection trajectory, we can construct three-dimensional distributions of ionospheric quantities, modified by the action of the ionospheric heater.

3 Presentation and discussion of results

The utilized mathematical model can describe different combinations of the solar cycle, geomagnetic activity level, and season. In the present study, the calculations are performed for autumn (5 November) and not high solar activity ($F_{10.7}$ =110) conditions under low geomagnetic activity (Kp=0). The spatial configuration of the electron and proton precipitation zones as well as intensities and average energies of the precipitating electrons and protons were chosen as consistent with the statistical model of Hardy et al. [31]. The thermospheric wind pattern is assumed to be a combination of theoretical and empirical models. This pattern is based on the experimental data on the neutral winds above 200 km at high latitudes [32].

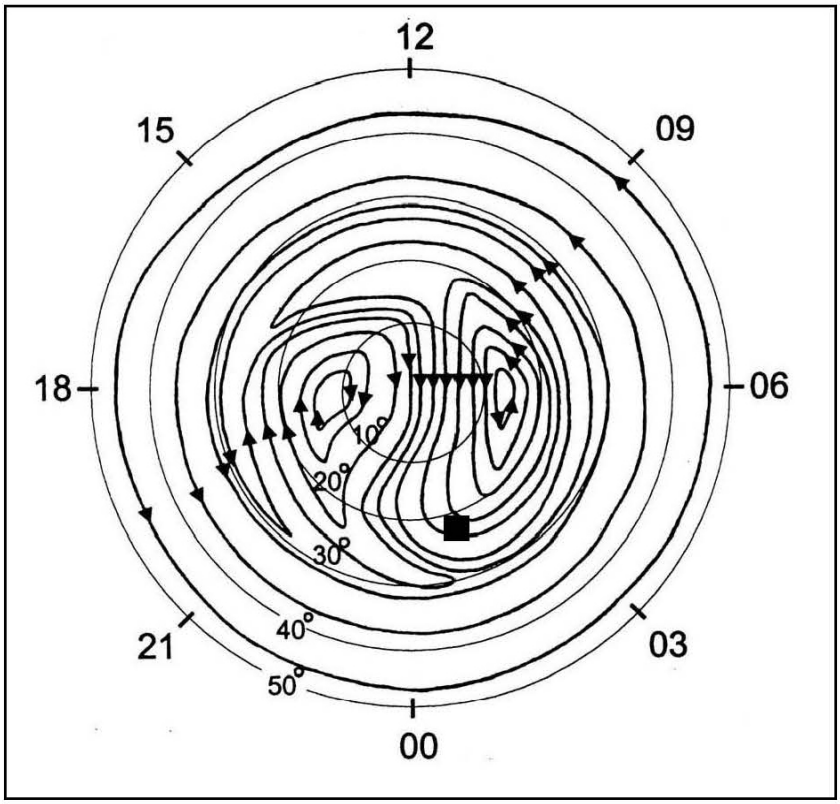

Figure 1: Plasma convection trajectories derived from the combination of the pattern *B* of the empirical convection models at polar latitudes of Heppner [28] and the empirical model of ionospheric electric fields at middle latitudes, developed by Richmond [29] and Richmond et al. [30]. Trajectories are depicted in the fixed sun-earth reference frame. Magnetic local time (MLT) and magnetic colatitude (ϑ) are indicated on the plot. The arrows indicate the direction of convection flows. The initial location of the ionospheric heater is indicated by the black square.

To examine how high-power high-frequency radio waves, pumped into the high-latitude ionosphere, influence on the ionospheric parameters distributions in the horizontal directions at F-layer altitudes, we made calculations for two distinct cases. For the first case, we obtained the distributions of the ionospheric

parameters under natural conditions without a powerful high-frequency wave effect. For the second case, the distributions of the ionospheric parameters were obtained on condition that an ionospheric heater, situated at the point with geographic coordinates of the HF heating facility near Tromso, Scandinavia, has been operated.

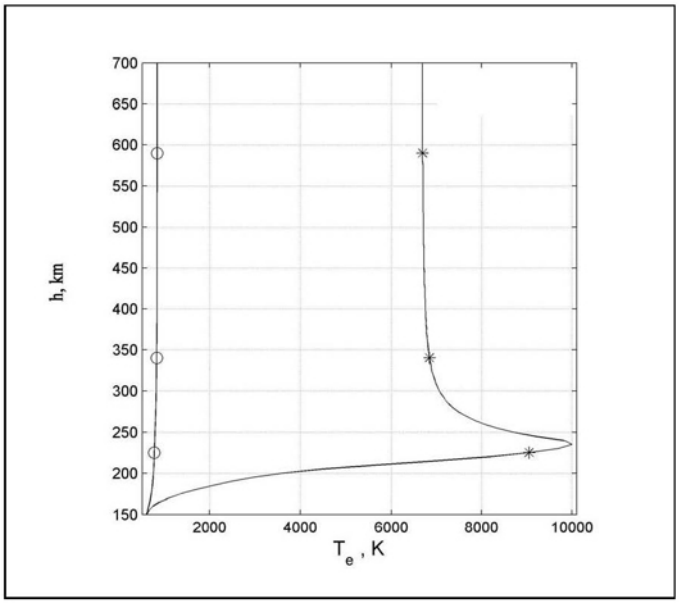

Figure 2: Profiles of the electron temperature versus distance from the Earth along the geomagnetic field line, situated in the illuminated region, obtained under natural conditions without artificial heating (left-hand curve) and disturbed by the heater at the moment of two minutes after turn on (right-hand curve).

For the second case, firstly, we made a series of calculations to choose the wave frequency which provides the maximal effect of HF heating on the electron concentration at the levels near to the F2-layer peak, that is, the most effective frequency for the large-scale F2-layer modification, f_{eff}, [21]. It was found that this most effective frequency is 2.6 MHz on condition that the maximal value of the effective absorbed power (EAP) is equal to 30 MW. Secondly, calculations were

carried out, using the pointed out values of the f_{eff} and EAP, to study how the HF radio waves affect the large-scale high-latitude F-layer modification. The ionospheric heater was supposed to operate during the period of five minutes, with the heater being located on the night side of the Earth on the magnetic meridian of 01.20 MLT. The initial location of the ionospheric heater is indicated by the square in Figure 1.

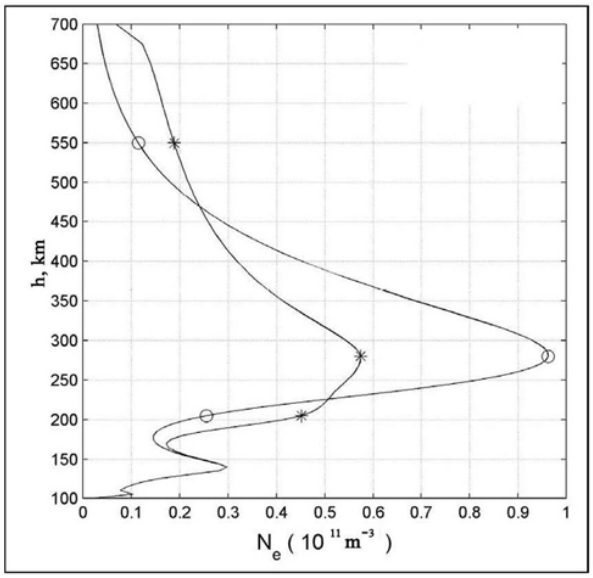

Figure 3: Profiles of the electron concentration versus distance from the Earth along the geomagnetic field line, situated in the illuminated region, obtained under natural conditions without artificial heating (marked by the symbol ○) and disturbed by the heater at the moment of approximately four minutes after turn on (marked by the symbol *).

The results of simulations are presented in Figures 2-6. The simulation results confirm the results obtained earlier in the studies of Mingaleva et al. [22 - 24] and devoted to investigation of how high-power high-frequency radio waves, pumped into the ionosphere, influence on the variations of height profiles of the ionospheric parameters at F-layer altitudes. Results of simulation indicated that a

great energy input from the powerful HF wave arises at the level, where the wave frequency is close to the frequency of the electron hybrid resonance, when the ionospheric heater is turned on and operates. At this level, as it is well seen from Figure 2, pronounced peak arises in the electron temperature profile. At this peak, the electron temperature can increase for some thousands of degrees. The increase in the electron temperature results in a rise in the electron gas pressure. From the level where the electron gas pressure peak is located, the upward and downward electron gas fluxes arise. Due to the electrical neutrality of the ionospheric plasma, the ion gas begins to move, too (plasma ambipolar transport). Thus, ionospheric plasma fluxes arise from the level where the maximum energy input from the powerful HF wave takes place. Owing to these fluxes, a visible decrease in the electron concentration profile can arise not only near the level of maximum energy absorption from the powerful HF wave, but also near the F2-layer peak (Figure 3). It is seen that powerful HF waves lead to the decrease of more than 40% in electron concentration at the level of the F2-layer peak. After turning off of the heater, the electron temperature decreases due to elastic and inelastic collisions between electrons and other particles of ionospheric plasma, and a period of recovery comes.

It is supposed that the ionospheric heater provides a beam width of 14.5^{o} (such as the beam width of the ionospheric high-frequency heating facility near Tromce, Scandinavia [33]). Therefore, the diameter of the illuminated region is approximately 88 km at 300 km altitude. One of specific features characteristic for the high-latitude ionosphere is the convection of the ionospheric plasma at F-layer altitudes. As a consequence of the convection, the volume of plasma, disturbed by a powerful HF wave, can abandon the region illuminated by an ionospheric heater. Therefore, the horizontal section of disturbed region at F-layer altitudes can differ from the horizontal section of the region illuminated by the heater.

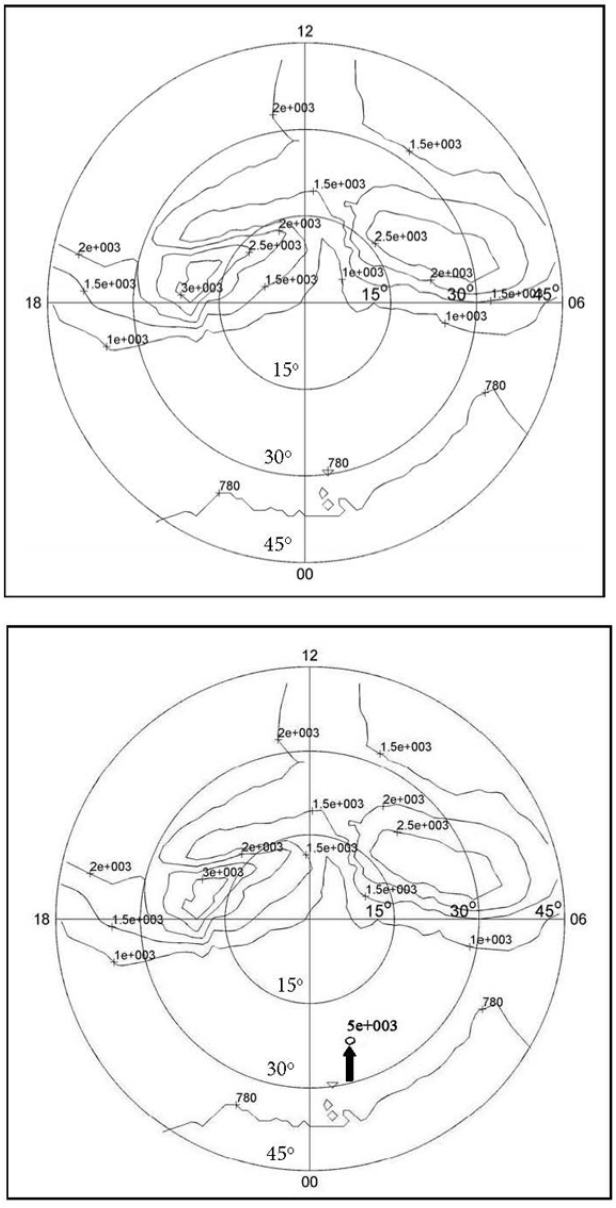

Figure 4: Simulated distributions of the electron temperature (K) at level of 280 km obtained under natural conditions without artificial heating (top panel) and obtained on condition that the ionospheric heater has been operated during the period of five minutes (bottom panel). The electron temperature hot spot, created artificially, is indicated by black pointer at the bottom panel.

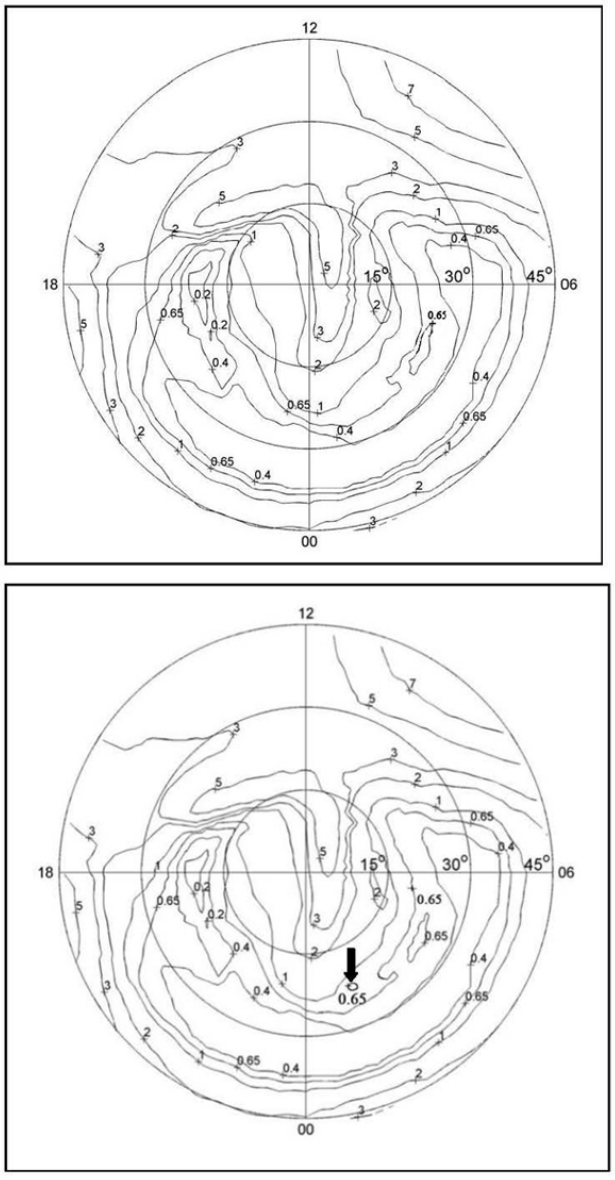

Figure 5: Simulated distributions of the electron concentration (in units of 10^{11} m^{-3}) at level of 320 km obtained under natural conditions without artificial heating (top panel) and obtained on condition that the ionospheric heater has been operated during the period of five minutes (bottom panel). The electron concentration cavity, created artificially, is indicated by black pointer at the bottom panel.

Let us consider the simulated spatial distributions of the ionospheric parameters. These distributions are presented in Figures 4-6. The simulation results, obtained under natural conditions without artificial heating, contain various large-scale inhomogeneous structures characteristic for the high-latitude ionosphere. The electron concentration distributions contain the well-known tongue of ionization, extended from the local noon side of the Earth across the polar cap to the night side, as well as the main ionospheric trough on the night side of the Earth (Figure 5). Simulated distributions of the electron concentration in the magnetic meridian plane, lying across the ionospheric heater, obtained under natural conditions without artificial heating, contains the sections of the tongue of ionization at polar latitudes, auroral ionization peak, produced by precipitating auroral electron and proton fluxes at latitudes of 60-73^{o}, and main ionospheric trough at latitudes of 55-60^{o} (Figure 6). It can be seen that the electron temperature hot spots are formed in the main ionospheric trough in the dawn and dusk sectors (Figure 4). It may be noted that the model calculations have been performed under condition that the electron and ion heat fluxes from the magnetosphere into the ionosphere are absent. Therefore, the electron temperature hot spots, situated in the morning and evening sectors of the main ionospheric trough, have arisen owing to internal ionospheric processes by means of the formation mechanism identified by Mingaleva and Mingalev [25].

From the simulation results, obtained on condition that the ionospheric heater has been operated during the period of five minutes, it is seen that the electron temperature hot spot is formed on the night side in the vicinity of the location of the ionospheric heater (Figure 4). Inside this hot spot, the electron temperature increases for some thousands of degrees. Moreover, the electron concentration cavity is formed on the night side in the vicinity of the location of the ionospheric heater (Figures 5 and 6). Inside this cavity, powerful HF waves lead to a decrease of about 40% in the electron concentration at the level of the F2-layer peak.

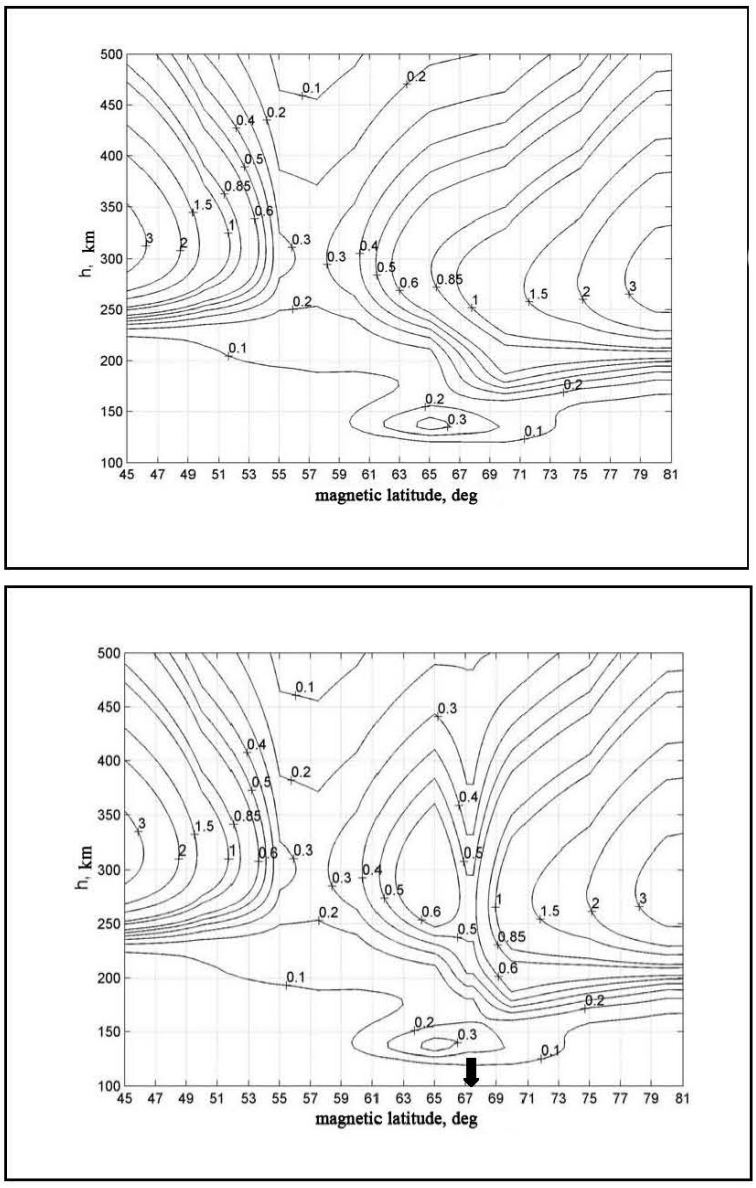

Figure 6: Simulated distributions of the electron concentration (in units of 10^{11} m^{-3}) in the magnetic meridian plane, lying across the ionospheric heater, obtained under natural conditions without artificial heating (top panel) and obtained on condition that the ionospheric heater has been operated during the period of five minutes (bottom panel). The location of the heater is indicated by the black pointer at the bottom panel.

The simulation results indicate that the cross sections of the artificial electron temperature hot spot and artificial electron concentration cavity have dimensions of about 100-150 km in the horizontal directions at the levels of the F layer (Figures 4-6). These dimensions are much less than the horizontal sizes of the natural large-scale inhomogeneous structures characteristic for the high-latitude ionosphere, in particular, of the natural electron temperature hot spots and main ionospheric trough. It is seen that the horizontal section of the region, disturbed artificially, at F-layer altitudes is more than the horizontal section of the region illuminated by the heater. This peculiarity is conditioned by the convection of the ionospheric plasma. The dimension of the artificial electron concentration cavity in the direction of the magnetic field line is about some hundreds of kilometers (Figure 6).

4 Conclusions

The mathematical model of the high-latitude ionosphere, developed earlier, was utilized to calculate three-dimensional distributions of ionospheric parameters, modified by the action of an ionospheric heater. The model is based on numerical solution of the system of transport equations, which consists of the continuity equation, equation of motion for ion gas, and heat conduction equations for ion and electron gases. The equations provide for the direct and resonantly scattered EUV solar radiation, energy-dependent chemical reactions, frictional force between ions and neutrals, accelerational and viscous forces of ion gas, thermal conductions of electron and ion gases, heating due to ion-neutral friction, Joule heating, heating due to solar EUV photons, heating caused by the action of the powerful HF radio waves, and electron energy losses due to elastic and inelastic collisions. The model takes into account the magnetization of the plasma at F-layer altitudes, drift of the ionospheric plasma, and geomagnetic field

inclination. Therefore, it may be expected that the model allows us to evaluate correctly the influence of the absorbed energy of heating HF waves on the large-scale F-region modification.

Firstly, we simulated the distributions of the ionospheric parameters under natural conditions without a powerful high-frequency wave effect. Secondly, the distributions of the ionospheric parameters were calculated on condition that an ionospheric heater, situated at the point with geographic coordinates of the HF heating facility near Tromso, Scandinavia, has been operated during the period of five minutes, with the heater being located on the night side of the Earth.

The simulation results, obtained under natural conditions without a powerful high-frequency wave effect, have reproduced the remarkable features of the high-latitude ionosphere such as the tongue of ionization, main ionospheric trough, auroral ionization peak, and electron temperature hot spots in the morning and evening sectors of the main ionospheric trough. It was found that the latter hot spots arise owing to internal ionospheric processes by means of the formation mechanism identified by Mingaleva and Mingalev [25].

The results of simulation, obtained on condition that the ionospheric heater has been operated during the period of five minutes, using the most effective frequency for the large-scale F2-layer modification, have indicated that artificial heating of the ionosphere by powerful HF waves ought to influence noticeably on the spatial structure of the nighttime high-latitude F-region ionosphere. In particular, the electron temperature hot spot was formed on the night side in the vicinity of the location of the ionospheric heater, with the electron temperature having increased for some thousands of degrees inside this hot spot. The electron concentration cavity was formed on the night side in the vicinity of the location of the ionospheric heater. Powerful HF waves led to a decrease of about 40% in the electron concentration at the level of the F2-layer peak inside this cavity. The cross sections of the artificial electron temperature hot spot and artificial electron concentration cavity have dimensions of about 100-150 km in the horizontal

directions at the levels of the F layer. These cross sections are more than the horizontal section of the region, illuminated by the heater, due to the convection of the high-latitude ionospheric plasma. The artificial electron concentration cavity is stretched in the direction of the magnetic field line for some hundreds of kilometers.

Acknowledgements. This work was partly supported by Grant No. 13-01-00063 from the Russian Foundation for Basic Research.

References

[1] W.F. Utlaut and E.J. Violette, A summary of vertical incidence radio observations of ionospheric modification, *Radio Science*, **9**, (1974), 895-903.

[2] W.E. Gordon and H.C. Carlson, Arecibo heating experiments, *Radio Science*, **9**, (1974), 1041-1047.

[3] G.P. Mantas, H.C. Carlson and C.H. La Hoz, Thermal response of F-region ionosphere in artificial modification experiments by HF radio waves, *Journal of Geophysical Research*, **86**, (1981), 561-574.

[4] T.B. Jones, T.R. Robinson, P. Stubbe and H. Kopka, EISCAT observations of the heated ionosphere, *Journal of Atmospheric and Terrestrial Physics*, **48**, (1986), 1027-1035.

[5] F.T. Djuth, B. Thide, H.M. Ierkic and M.P. Sulzer, Large F-region electron-temperature enhancements generated by high-power HF radio waves, *Geophysical Research Letters*, **14**, (1987), 953-956.

[6] L.M. Duncan, J.P. Sheerin and R.A. Behnke, Observations of ionospheric cavities generated by high-power radio waves, *Physical Review Letters*, **61**, (1988), 239-242.

[7] J.D. Hansen, G.J. Morales, L.M. Duncan and G. Dimonte, Large-scale HF-induced ionospheric modification: experiments, *Journal of Geophysical Research*, **97**, (1992), 113-122.

[8] G.P. Mantas, Large 6300-Å airglow intensity enhancements observed in ionosphere heating experiments are exited by thermal electrons, *Journal of Geophysical Research*, **99**, (1994), 8993-9002.

[9] F. Honary, F., A.J. Stocker, T.R. Robinson, T.B. Jones and P. Stubbe, Ionospheric plasma response to HF radio waves operating at frequencies close to the third harmonic of the electron gyrofrequency, *Journal of Geophysical Research*, **100**, (1995), 21489-21501.

[10] T.R. Robinson, F. Honary, A.J. Stocker, T.B. Jones and P. Stubbe, First EISCAT observations of the modification of F-region electron temperatures during RF heating at harmonics of the electron gyro frequency, *Journal of Atmospheric and Terrestrial Physics*, **58**, (1996), 385-395.

[11] B. Gustavsson, T. Sergienko, M.T. Rietveld, F. Honary, A. Steen, B.U.E. Brandstrom, T.B. Leyser, A.L. Aruliah, T. Aso, M. Ejiri and S. Marple, First tomographic estimate of volume distribution of HF-pump enhanced airglow emission, *Journal of Geophysical Research*, **106**, (2001), 29105-29124.

[12] M.T. Rietveld, M.J. Kosch, N.F. Blagoveshchenskaya, V.A. Kornienko, T.B. Leyser and T.K. Yeoman, Ionospheric electron heating, optical emissions, and striations induced by powerful HF radio waves at high latitudes: Aspect angle dependence, *Journal of Geophysical Research*, **108**(A4), (2003), 1141, doi:10.1029/2002JA009543.

[13] M. Ashrafi, M.J. Kosch, K. Kaila, and B. Isham, Spatiotemporal evolution of radio wave pump-induced ionospheric phenomena near the fourth electron gyroharmonic, *Journal of Geophysical Research*, **112**(A5), (2007), A05314, doi:10.1029/2006JA011938.

[14] R.S. Dhillon, T.R. Robinson and T.K. Yeoman, EISCAT Svalbard radar observations of SPEAR-induced E- and F-region spectral enhancements in the polar cap ionosphere, *Ann. Geophys*., **25**, (2007), 1801-1814.

[15] M.J. Kosch, T. Pedersen, M.T. Rietveld, B. Gustavsson, S.M. Grach and T. Hagfors, Artificial optical emissions in the high-latitude thermosphere induced by powerful radio waves: An observational review, *Adv. Space Res.*, **40**, (2007), 365-376.

[16] T.K. Yeoman, N. Blagoveshchenskaya, V. Kornienko, T.R. Robinson, R.S. Dhillon, D.M. Wright and L.J. Baddeley, SPEAR: Early results from a very high latitude ionospheric heating facility, *Adv. Space Res*., **40**, (2007), 384-389.

[17] L.B.N. Clausen, T.K. Yeoman, D.M. Wright, T.R. Robinson, R.S. Dhillon and S.C. Gane, First results of a ULF wave injected on open field lines by Space Plasma Exploration by Active Radar (SPEAR), *Journal of Geophysical Research*, **113**(A1), (2008), A01305, doi:10.1029/2007JA012617.

[18] T. Pedersen, R. Esposito, E. Kendall, D. Sentman, M. Kosch, E. Mishin and R. Marshall, Observations of artificial and natural optical emissions at the HAARP facility, *Ann. Geophys*., **26**, (2008), 1089-1099.

[19] G.I. Mingaleva and V.S. Mingalev, Response of the convecting high-latitude F layer to a powerful HF wave, *Ann. Geophys*., **15**, (1997), 1291-1300.

[20] G.I. Mingaleva and V.S. Mingalev, Modeling the modification of the nighttime high-latitude F-region by powerful HF radio waves, *Cosmic Research*, **40**(1), (2002), 55-61.

[21] G.I. Mingaleva and V.S. Mingalev, Simulation of the modification of the nocturnal high-latitude F layer by powerful HF radio waves, Geomagnetism and Aeronomy, **43**(6), (2003), 816-825 (Russian issue).

[22] G.I. Mingaleva, V.S. Mingalev and I.V. Mingalev, Simulation study of the high-latitude F-layer modification by powerful HF waves with different frequencies for autumn conditions, Ann. Geophys., **21**, (2003), 1827-1838.

[23] G.I. Mingaleva, V.S. Mingalev and I.V. Mingalev, Model simulation of the large-scale high-latitude F-layer modification by powerful HF waves with different modulation, *J. Atmos. Sol.-Terr. Phys*., **71**, (2009), 559-568.

[24] G.I. Mingaleva, V.S. Mingalev and O.V. Mingalev, Simulation study of the large-scale modification of the mid-latitude F-layer by HF radio waves with different powers, *Ann. Geophys*., **30**, (2012), 1213–1222, doi:10.5194/angeo-30-1213-2012.

[25] G.I. Mingaleva and V.S. Mingalev, The formation of electron temperature hot spots in the main ionospheric trough by the internal processes, *Ann. Geophys*., **14**, (1996), 816-825.

[26] G.I. Mingaleva and V.S. Mingalev, *Three-dimensional mathematical model of the polar and subauroral ionosphere*, in *Modeling of the upper polar atmosphere processes*, (eds. V.E. Ivanov, Ya.A. Sakharov, and N.V. Golubtsova), PGI, Murmansk, (1998), 251-265 (in Russian).

[27] N.Sh. Blaunshtein, V.V. Vas'kov and Ya.S. Dimant, Resonance heating of the F region by a powerful radio wave, *Geomagnetism and Aeronomy*, **32**(2), (1992), 95-99 (Russian issue).

[28] J.P. Heppner, Empirical models of high-latitude electric fields, *Journal of Geophysical Research*, **82**, (1997), 1115- 1125.

[29] A.D. Richmond, Electric field in the ionosphere and plasmasphere on quiet days, *Journal of Geophysical Research*, **81**, (1976), 1447-1450.

[30] A.D. Richmond, M. Blanc, B.A. Emery, R.H. Wand, B.G. Fejer, R.F. Woodman, S. Ganguly, P. Amayenc, R.A. Behnke, C. Calderon and J.V. Evans, An empirical model of quiet-day ionospheric electric fields at middle and low latitudes, *Journal of Geophysical Research*, **85**, (1980), 4658-4664.

[31] D.A. Hardy, M.S. Gussenhoven and D. Brautigam, A statistical model of auroral ion precipitation, *Journal of Geophysical Research*, **94**, (1989), 370-392.

[32] J.M. Meriwether, J. P. Heppner, J.D. Stolaric and E.M. Wescott, Neutral winds above 200 km at high latitudes, *Journal of Geophysical Research*, **78**, (1973), 6643-6661.

[33] M.T. Rietveld, H. Kohl, H. Kopka and P. Stubbe, Introduction to ionospheric heating at Tromso - 1.Experimental overview, *Journal of Atmospheric and Terrestrial Physics*, **55**, (1993), 577-599.